# LIQUID-SIDE INTERFACIAL HEAT TRANSFER IN INVERTED ANNULAR FILM BOILING

**J. M. Kelly**
U.S. Nuclear Regulatory Commission,
MS: CS03-07m, Washington, DC 20555, USA
Joseph.Kelly@NRC.gov

## ABSTRACT

A constitutive model for liquid-side interfacial heat transfer is necessary for a two-fluid description of the inverted annular film boiling (IAFB) regime. The experimental database for this interfacial heat transfer phenomena is very limited and contains no data for the rod bundle geometries of interest in reactor safety analysis. An analysis procedure was developed that allows the determination of this quantity from the reflood experiments conducted in the Rod Bundle Heat Transfer (RBHT) Test Facility that is operated for the NRC by the Pennsylvania State University.

For RBHT high flooding rate reflood tests, a quasi-steady analysis procedure was used to translate the measured fluid temperature histories into axial profiles of the liquid temperature for the IAFB region. The local values of the liquid-side interfacial heat transfer coefficient were then determined as a function of the subcooling downstream of the quench front. At high values of the subcooling, where the vapor-liquid interface is expected to be smooth, the liquid-side Nusselt number approached an asymptotic value of about $130 \cdot Pr_l^{1/2}$ for the conditions of these tests (G ~ 155 kg/m$^2$s, and 0.138 ≤ P (MPa) ≤ 0.414). Further downstream of the quench front, as the subcooling decreased, the Nusselt number increased dramatically as the vapor flow increased and the surface became wavy.

**KEYWORDS**
Inverted annular film boiling, interfacial heat transfer, TRACE, RBHT, two-fluid model

## 1. INTRODUCTION

The U.S. Nuclear Regulatory Commission (NRC) system level thermal-hydraulic analysis code TRACE (TRAC/RELAP Advanced Computational Engine) is being developed to provide a best-estimate analysis capability for operating pressurized- and boiling-water reactors as well as the next generation of evolutionary light-water reactor designs. One of the experiments used to support TRACE model development is the Rod Bundle Heat Transfer (RBHT) Test Facility operated for the NRC by the Pennsylvania State University. Data from high flooding rate RBHT reflood tests were used to quantify the liquid-side interfacial heat transfer.

Inverted annular film boiling (IAFB) occurs during the reflooding of a light water reactor core when the liquid is significantly subcooled and the resulting precursory cooling governs the quench rate. In addition, high-pressure IAFB may occur during an Anticipated Transient Without Scram (ATWS) event if regions of a boiling water reactor core exceed the critical heat flux during power oscillations. In the IAFB regime, only a thin vapor film separates the hot surface from the subcooled liquid core and the heat transfer paths are as depicted in Figure 1 below. Most of the heat transfer from the wall is across the vapor film to the saturated liquid interface. The subsequent transfer of heat from the interface to the subcooled liquid core, i.e. $Q_{li}$, suppresses the vapor generation rate thereby allowing for a thin vapor film and relatively large film boiling heat transfer coefficients.

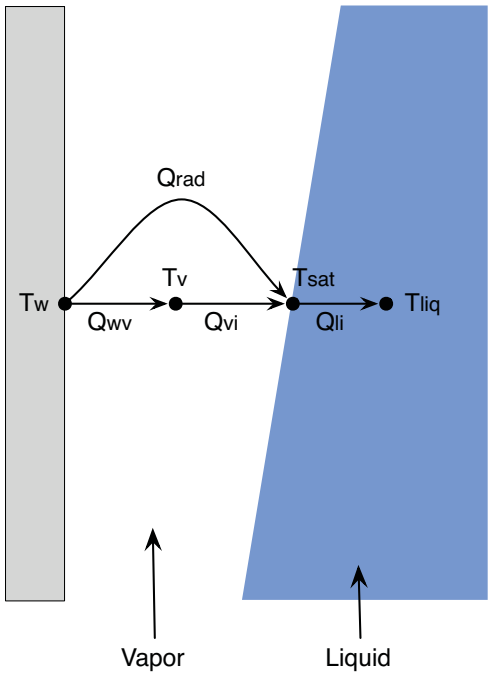


**Figure 1. Schematic of heat transfer paths for inverted annular film boiling.**

From a literature survey, four experiments were identified where there was an attempt to measure the liquid-side interfacial heat transfer. The first was for pool film boiling of water at atmospheric pressure on a vertical plate conducted by UCLA [1, 2]. Here the interfacial heat transfer rate was determined using holographic interferometry to measure the temperature profile in the liquid pool. The level of subcooling was modest, $\Delta T_{sub} < 7$ °K, and only five values for the average interfacial heat transfer coefficient were reported with values ranging from about 4,000 to 10,000 ($W/m^2K$).

Takenaka [3, 4] and Aritomi [5] both conducted steady-state film boiling experiments in a tube using a hot patch to stabilize the quench front with Freon R-113 as the coolant. Takenaka measured the temperature of the inverted annular liquid core near the test section outlet and used the temperature rise of the liquid core to select a model for the interfacial heat transfer coefficient. For their low Reynolds number conditions, $Re_l \sim 5300$, the inferred heat transfer rate was about six times larger than that given by the Dittus-Boelter equation for fully developed forced turbulent convection in tubes.

Aritomi [5] measured the velocity profile of the inverted annular liquid core and used this to determine the vapor film thickness. From this value of the vapor film thickness, an estimate of the vapor flow rate was made and used to infer the interfacial heat transfer rate. An empirical correlation was proposed for the liquid-side interfacial heat transfer coefficient but was noted to be strictly limited to Freon-113 at atmospheric pressure and for the range of conditions used in their experiments.

Finally, Meduri [6] investigated both the effects of mass flux and liquid subcooling upon IAFB for water at atmospheric pressure in a vertical flow channel with the heated surface being a vertical flat plate. The liquid-side interfacial heat transfer rate was inferred from measurements of the liquid temperature profile normal to the vapor-liquid interface made using traversing micro-thermocouples. The results evinced little effect of either the mass flux or entrance length. However, the interfacial heat transfer coefficient appeared to be strongly dependent upon the value of the liquid subcooling, having an asymptotic value for $\Delta T_{sub} > 15$ °K and increasing exponentially as the subcooling decreased and the interface became rough.

## 2. RBHT FACILITY AND TEST CONDITIONS

As part of the U.S. Nuclear Regulatory Commission's safety analysis computer code development efforts, the Rod Bundle Heat Transfer (RBHT) Test Facility was designed and constructed at The Pennsylvania State University. The RBHT Test Facility is a full-length simulation of a portion of a pressurized water reactor (PWR) fuel assembly. The bundle is a 7x7 rod array with four unheated corner rods and 45 heated electrical rods that simulates a 17x17 PWR fuel assembly. The RBHT bundle has a heated length of 3.66 m, with typical PWR rod diameters of 9.5 mm and a rod pitch of 12.6 mm. The heater rods have a top skewed power shape with a peak to average power of 1.5 at the 2.74 m elevation. Prototypical PWR mixing vane spacer grids were simulated at seven axial locations.

A detailed description of the RBHT facility and its instrumentation is documented in Rosal et al. [7] and Hochreiter et al. [8]. This experimental program was designed to provide data suitable for TRACE model development, so the instrumentation, test conditions and procedures were tailored to facilitate model development activities. Specifically:

- The RBHT experiments were performed with constant power vs. time, as opposed to simulating the decay power curve. This extends the reflood transient and allows for data analysis of quasi-steady conditions without the additional complication of a rapidly moving quench front.
- A total of 256 rod thermocouples were installed at 59 axial elevations so that a comprehensive picture of the axial temperature profile is provided. This is key in allowing for the accurate calculation of the quench front position and velocity necessary for the quasi-steady analysis.
- A total of 54 fluid thermocouples were installed at 19 axial elevations. These were downwards facing miniature fast-response thermocouples located at the subchannel centerline.
- A total of 23 differential pressure measurements were included to provide the axial profile of void fraction within the bundle during reflood. In the region of interest for IAFB, the axial measurement spans were between 7.6 and 12.7 cm.

A total of 25 valid reflood experiments were performed in the RBHT facility covering a range of flooding rates from 2.54 to 15.24 cm/s. Of these, five tests targeted the IAFB regime and were used to quantify the liquid-side interfacial heat transfer for the subcooled liquid core, see Table 1.

**Table 1. RBHT reflood test conditions used for IAFB analysis**

| RBHT Test # | Pressure [kPa] | Flooding Rate [m/s] | Peak Power [kW/m] | Initial Peak Cladding Temperature [°K] | Inlet Subcooling [°K] |
|---|---|---|---|---|---|
| **1143** | 138 | 0.152 | 2.3 | 1144 | 83 |
| **1280** | 138 | 0.154 | 2.3 | 1139 | 83 |
| **1285** | 276 | 0.155 | 2.3 | 1143 | 84 |
| **1291** | 414 | 0.155 | 2.3 | 1145 | 83 |
| **1300** | 276 | 0.078 | 2.3 | 1148 | 75 |

## 3. RBHT DATA ANALYSIS

Although designed to measure the superheated vapor temperature in the dispersed flow film boiling regime, the RBHT fluid thermocouples are also capable of measuring the subcooled liquid core temperature in IAFB. Figure 2 gives examples of both the rod and steam probe thermocouple histories for RBHT reflood test #1143. The region of interest is labeled "subcooled film boiling" and persists from about 54 to 66 seconds. Figure 3 is a close-up look at the measured fluid temperature for the subcooled film-boiling region. As shown in this figure, about half of the liquid subcooling is extinguished by the quench front heat release with the remaining heat up being the result of interfacial heat transfer.

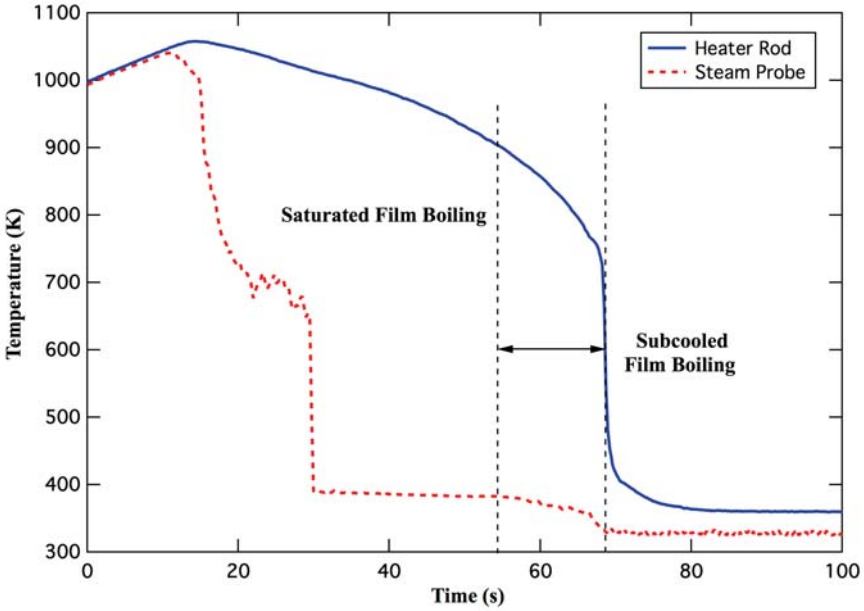


**Figure 2. Example of rod and steam probe temperature histories for RBHT reflood test #1143.**

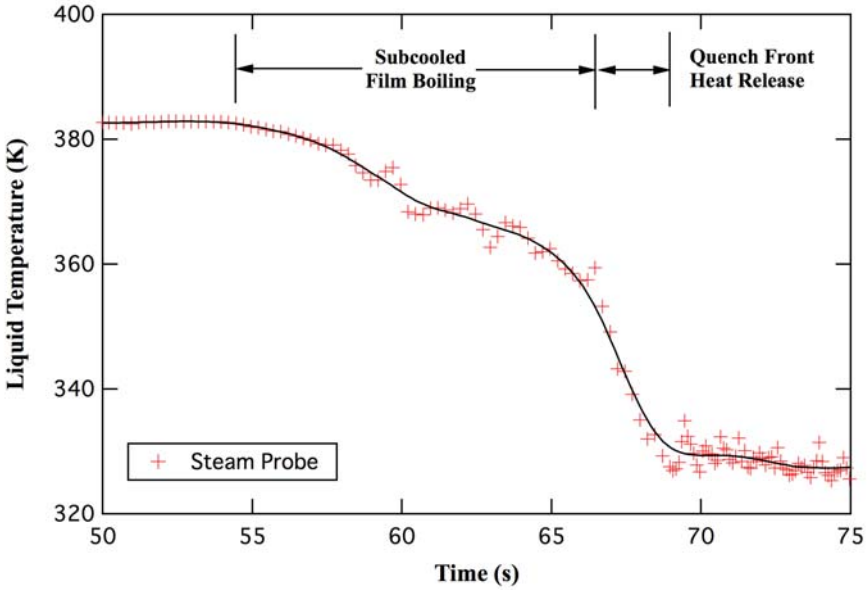


**Figure 3. Fluid temperature history for the 1.524 m elevation of RBHT reflood test #1143.**

For the RBHT reflood tests, the quench front velocity is about an order of magnitude less than the liquid velocity. This allows the use of a quasi-steady analysis technique where the frame of reference is a Lagrangian one that moves with the quench front. Time histories are then translated into axial profiles by

$$\Delta Z_{QF} = \int_{\Delta t} V_{QF} \cdot dt \tag{1}$$

With this transformation and the local value of the saturation temperature, the liquid temperature history shown above in Figure 3 can be converted into liquid subcooling as a function of distance from the quench front as shown below in Figure 4.

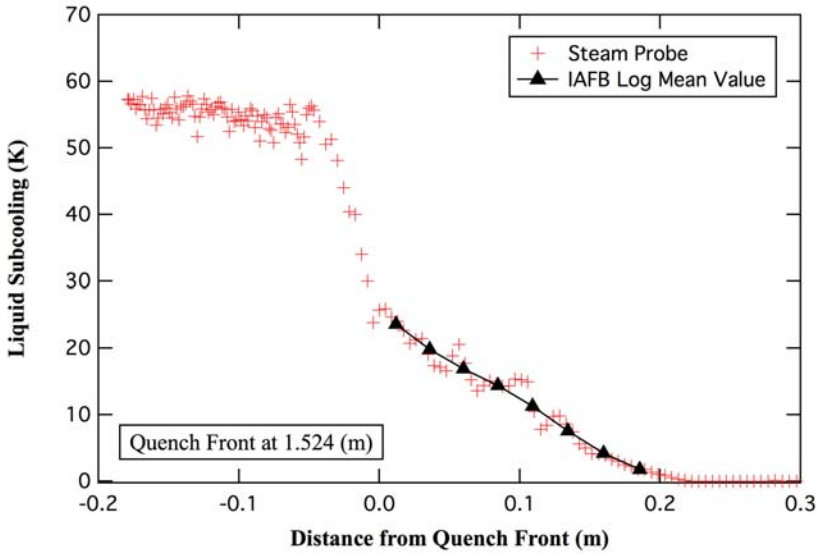


**Figure 4. Example of fluid temperature history transformed to axial profile of subcooling.**

The axially averaged value of the interfacial heat transfer coefficient at the surface of the subcooled liquid column is then calculated from the formula for a heat exchanger with the hot side at a fixed temperature,

$$\overline{h}_{li} = \left( \frac{G_l \cdot A \cdot C_{P,l}}{A_i} \right) \cdot \ln\left( \frac{\Delta T_1}{\Delta T_2} \right) \tag{2}$$

where the temperature differences in equation (2) refer to the local subcooling at that point (see Takahashi et al., [20]). Considering the geometry of the liquid core region to be circular then gives the liquid-side Nusselt number for the interval between points "1" and "2" as

$$\overline{Nu}_{li} = \left( \frac{G_l \cdot A \cdot C_{P,l}}{\pi \cdot \Delta Z_{12} \cdot k_l} \right) \cdot \ln\left( \frac{\Delta T_1}{\Delta T_2} \right) \tag{3}$$

In Figure 4 the subcooled IAFB region extends from the quench front to a distance of about 0.2 m downstream. A smoothing algorithm was used to filter the noise in the thermocouple signal and this region was subdivided into intervals of about 2.5 cm in length with the log mean temperature calculated for each. Equation (3) was then used to calculate the local values of the liquid-side Nusselt number for each interval as shown below in Figure 5 for the two fluid thermocouples at this elevation.

The behavior depicted in Figure 5 has a few interesting features. First, there is no obvious entrance length effect for the region immediately downstream of the quench front as is supposed in most two-fluid models. Instead, the Nusselt number appears to have reached an asymptotic value of about 200 that remains relatively constant for about half of the subcooled IAFB region. Further downstream, as the subcooling is reduced and the vapor flow increases, the interface becomes wavy and the liquid column may begin to oscillate within the channel as observed by Costigan and Wade [9]. The result is the dramatic increase in the liquid-side Nusselt number as the subcooled liquid column approaches saturation in agreement with the effect noted for the UCLA vertical plate tests [6] discussed above.

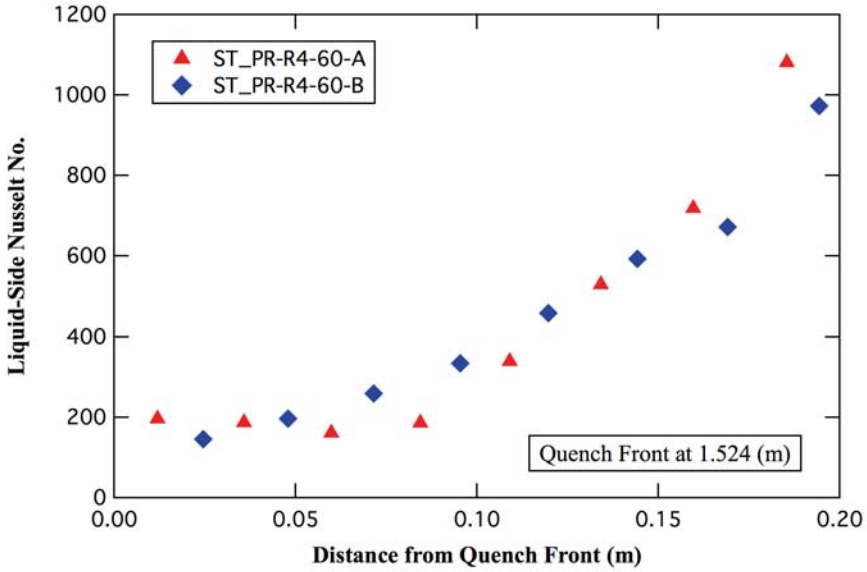


**Figure 5. Example of axial profile of the liquid-side Nusselt number for RBHT test #1143[1].**

This analysis was conducted all of the tests listed in Table 1 for every valid fluid thermocouple for which the signal was not too noisy. This noise was most likely due to oscillations of the liquid column within the subchannel exposing the tip of the thermocouple probe to temperatures ranging from the maximum subcooling at the column centerline to the warmer fluid near the interface. The smoothing of the thermocouple signal to ascertain the log mean temperature difference for each subinterval is the primary contributor to the error in $Nu_{li}$, which based on the variance of the data, is estimated to be ±40%.

All of the values of the liquid-side Nusselt number deduced for reflood test #1143 are shown below in Figure 6 as a function of the liquid subcooling. The asymptotic limit at high subcooling, where the interface is expected to be relatively smooth, is clearly shown and has a value of 181 ± 36. This apparent exponential dependence upon subcooling for test #1143 was consistent for all of the RBHT high flooding reflood tests.

Table 2 gives the values of the liquid-side Nusselt number at the high subcooling asymptotic limit for the four tests with a flooding rate of about 15 cm/s. The lower flooding rate test #1300 had most of the subcooling extinguished by the quench front heat release so that only nine values for $Nu_{li}$ were obtained

[1] The instrument tag ST_PR-R4-60-A corresponds to a steam probe on rake #4 located at the 60 inch (1.524 m) elevation located in a subchannel within the centermost row of the bundle. The tag ending with "B" indicates a steam probe located one row away from the center.

at relatively low values of the subcooling and so the asymptotic limit was not reached. This prevented an investigation of the mass flux effect upon the interfacial heat transfer from the RBHT test data.

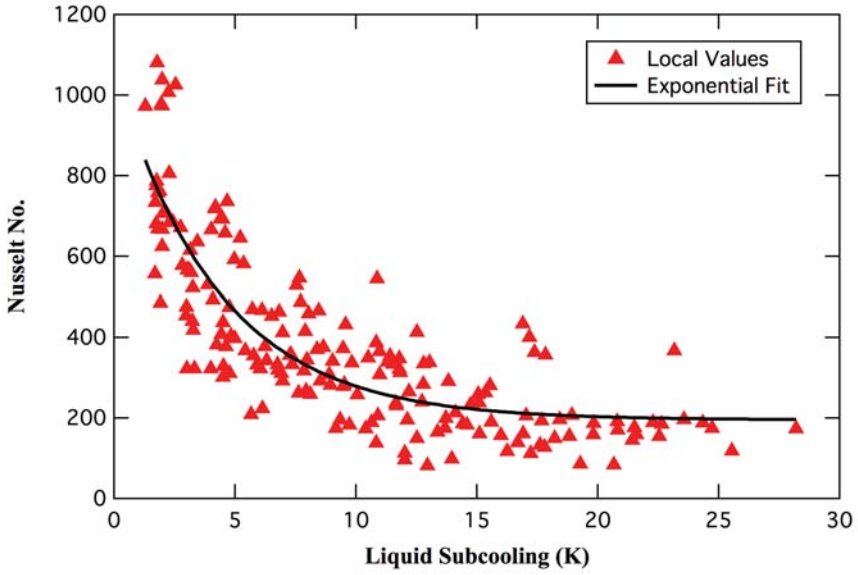


**Figure 6. Liquid-side Nusselt numbers for RBHT reflood test #1143.**

Reflood tests were conducted at three pressure levels and showed a slight tendency for the liquid-side Nusselt number to decrease as the pressure increased. For turbulent heat transfer at a free surface, the liquid-side Nusselt number is expected to be proportional to the square root of the liquid Prandtl number. When exponential fits of the ratio $Nu_{li}/Pr_l^{1/2}$ were compared, data from three of the tests in Table 2 collapsed into a single curve. However, the difference between the values for two tests conducted at the same nominal conditions, tests #1143 and #1280, are larger than the apparent pressure effect and so no definitive conclusion can be reached as the magnitude of the uncertainties is larger than the effect.

**Table 2. Effect of liquid Prandtl number on asymptotic values of the liquid-side Nusselt number.**

| Test No. | Pressure (bar) | Prandtl No. | $Nu_{li,\infty}$ | $Nu_{li,\infty}/Pr_l^{1/2}$ |
|---|---|---|---|---|
| 1143 | 1.38 | 1.87 | 181 ± 36 | 132 |
| 1280 | 1.38 | 1.87 | 149 ± 50 | 109 |
| 1285 | 2.76 | 1.50 | 161 ± 29 | 132 |
| 1291 | 4.14 | 1.33 | 156 ± 45 | 136 |

While the results of the RBHT data analysis effort has provided information on both the magnitude and behavior of the liquid-side interfacial heat transfer for the IAFB regime, the range of experimental conditions was not sufficient to determine its dependence upon either mass flux or pressure. To gain some insight into these possible parametric effects, two additional analysis methods were used to estimate the magnitude of the liquid-side Nusselt number as described in the next section.

## 4. SUPPLEMENTARY DATA ANALYSIS EFFORTS

To extend the mass flux and pressure range of the database, two supplementary data analysis procedures were used to obtain estimates of the liquid-side Nusselt for experiments where the interfacial heat transfer was not measured. The first of these was used in the original TRACE model development effort [10] to infer "maximum possible" values of $Nu_{li}$ from steady-state film boiling experiments where the quench front was stabilized using a hot patch. The liquid-side Nusselt number is given by

$$Nu_{li} = \frac{q_{li}''}{\Delta T_{sub}} \cdot \frac{D_c}{k_l} \tag{4}$$

However, in these experiments neither the liquid-interface heat flux nor the liquid subcooling was measured and so two assumptions were made: 1) the liquid-interface heat flux was approximated by that of the wall, and 2) the liquid subcooling was calculated from the equilibrium quality. Both assumptions are reasonable for the IAFB regime when the liquid is highly subcooled and the vapor generation rate is small but become increasingly poorer as the subcooling decreases. The first assumption serves to maximize the numerator of equation (4) while the second minimizes the denominator thereby generating an upper limit for the value of the liquid-side Nusselt number.

This analysis procedure was used for the atmospheric pressure tests of Fung [11] and the high-pressure tests conducted at Winfrith [12-14]. Figure 7 shows all of the values inferred from the tube experiment of Fung plotted as a function of subcooling and compares them to the exponential fit of the data values from the RBHT reflood test #1143. The first observation from Figure 7 is the surprisingly minimal effect of the mass flux upon the Nusselt number despite the variation of the liquid core Reynolds number from about 3700 to 19,000. The second is the remarkable agreement between these maximum inferred values and the data values from RBHT test #1143. Indeed, both the magnitude and behavior of the Nusselt number are well matched except at low values of the subcooling where the breakdown in the validity of the two assumptions used in estimating the maximum values occurs. Similar behavior was seen for the high-pressure Winfrith tube tests, with no clear mass flux effect observed even for a liquid core Reynolds number of 75,000. The observed pressure effect is discussed below in the "Model Development" section.

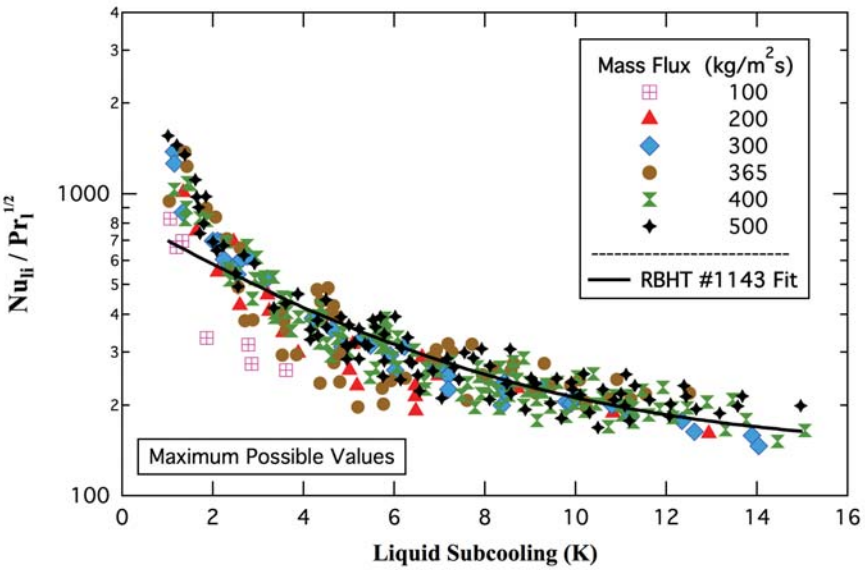


**Figure 7. Values for the liquid-side Nusselt number from Fung [11] tube film-boiling tests.**

The second data analysis method uses the dependence of the minimum film boiling point upon the liquid subcooling to estimate the interfacial heat transfer. The minimum film boiling point corresponds to the minimum heat flux condition in the boiling curve that separates the film boiling and transition boiling regimes. In steady-state film boiling experiments where the quench front has been stabilized by using a hot patch, the point at which the vapor film collapses can be determined by systematically reducing the test section power until spontaneous quenching occurs. The heat flux at the minimum film boiling point can be viewed as the superposition of two components:

$$q''_{min}\left(P,G,\Delta T_{sub}\right) \;=\; q''_{min,sat}\left(P,G\right) \;+\; \Delta q''_{min}\left(P,G,\Delta T_{sub}\right) \tag{5}$$

The first term on the right hand side of equation (5) is the value of the wall heat flux corresponding to the vapor generation rate necessary to prevent rewetting for saturated flow conditions at the specified values of pressure and mass flux. The second term is the increment in wall heat flux necessary to counteract the effect of the subcooled liquid core upon the vapor generation rate. Equating this increment to the liquid-side interfacial heat transfer rate yields

$$Nu_{li} \;\approx\; \left(\frac{D_h}{k_l}\right)\cdot\left(\frac{\Delta q''_{min}}{\Delta T_{sub}}\right) \tag{6}$$

so that an estimate of the Nusselt number can be obtained from the slope of the curve of the minimum film boiling heat flux versus subcooling.

Figure 8 gives an example of this data analysis technique for the tube film boiling experiment of Chen et al. [15] for a pressure of ~0.12 MPa and a mass flux range of 100 – 725 (kg/m$^2$s). All of the 17 subcooled data points fell near a straight line, from the slope of which the liquid-side Nusselt number was estimated as 175 ± 13. This gives a value of 126 for the ratio $Nu_{li}/Pr_l^{1/2}$ in substantial agreement with the values from the RBHT reflood tests. In addition to the experiments of Chen, estimates of the liquid-side Nusselt number were also obtained from the minimum film boiling point data from Fung [11] and Stewart [16]. This extended the interfacial heat transfer database to a pressure of 9 MPa and a mass flux of 2750 (kg/m$^2$s) as discussed in the "Model Development" section.

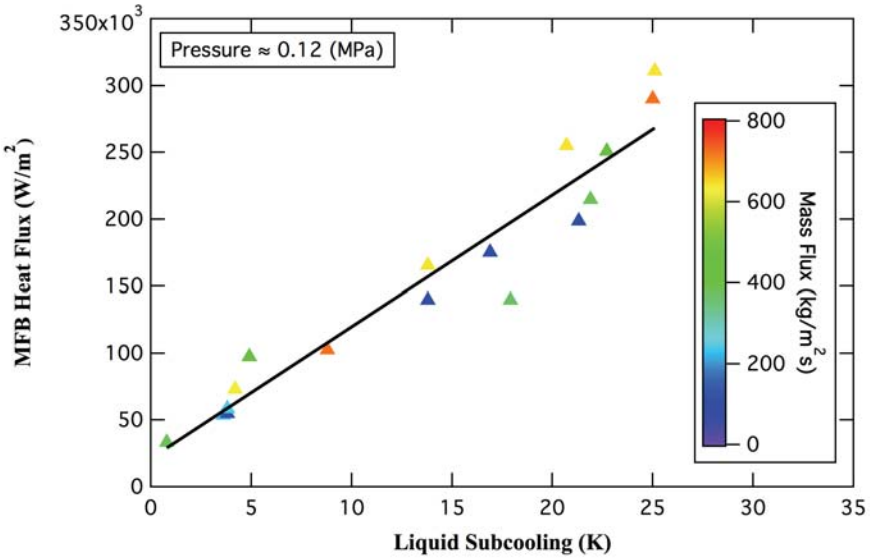


**Figure 8. Effect of subcooling on MFB heat flux for the tube experiments of Chen et al. [15].**

## 5. MODEL DEVELOPMENT EFFORT

Model development for the interfacial heat transfer in the IAFB regime is ongoing and this section describes the current effort to resolve the effects of void fraction, pressure, and mass flux. Figure 9 gives an example of the void fraction dependence of the liquid-side Nusselt number taken from the RBHT reflood test #1143. Just downstream of the quench front, at very low values of the void fraction where the interface is expected to be smooth and the subcooling is high, the Nusselt number approaches a constant value of about 200. This constant value might be the IAFB analog to that proposed by Saha & Zuber [17] for the "thermally controlled" regime in subcooled boiling. Saha & Zuber correlated the liquid-side Nusselt number for the flow of a subcooled liquid core flowing past a wall covered with a bubble layer. For the thermally controlled regime, they found that a constant value, $Nu_{li} = 455$, held for values of the Peclet number less than 70,000. Though larger in magnitude, as would be expected due to the differences in flow topology, this behavior is similar to that observed for the highly subcooled IAFB regime.

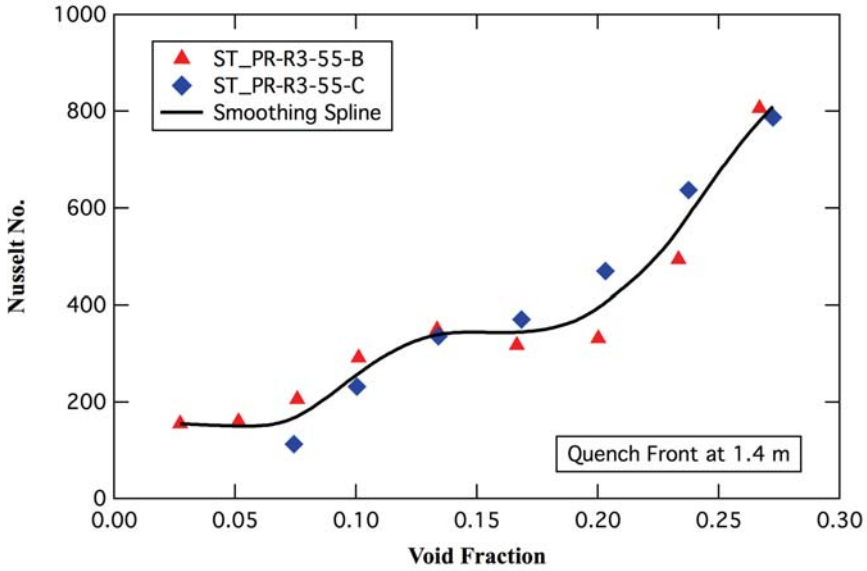


**Figure 9. Example of liquid-side Nusselt number dependence on void fraction for test #1143.**

As the void fraction increases above about 10%, the Nusselt number also increases to plateau at a value of about 350. This initial increase in the liquid-side Nusselt number might be the result of the enhancement of the turbulence level in the liquid core due to interfacial shear. For example, De Angelis et al. [18] expressed the mass transfer coefficient at an air-water interface due to the effects of interfacial shear as

$$K_{li} = 0.10 \cdot U_i \cdot Sc_l^{-1/2} \tag{7}$$

where $U_i$ is the interfacial friction velocity. Using the heat-mass transfer analogy, the liquid-side Nusselt number would be

$$Nu_{li} = 0.10 \cdot Re_t \cdot Pr_l^{1/2} \tag{8}$$

with the turbulence Reynolds number defined in terms of the interfacial friction velocity and the liquid core diameter. To evaluate $U_i$, the interfacial friction force is set equal to the buoyancy force and the liquid core is assumed to have a circular cross-section so that

$$U_i = \left[\tfrac{1}{4}\cdot\alpha\cdot(1-\alpha)^{1/2}\cdot g\cdot\Delta\rho\cdot D_h/\rho_l\right]^{1/2} \quad (9)$$

Combining these equations, an estimate for the liquid-side Nusselt number due to interfacial shear alone was calculated for the conditions of RBHT test RF-1143. Both the magnitude and shape of the curve for $Nu_{li}$ as a function of void fraction were well matched for the plateau region given in Figure 9 and so may form the basis for a model of this enhancement mode.

Further increases in the void fraction above about 20% result in a step rise in the Nusselt number as increases in the vapor flow cause the vapor-liquid interface to become rough and possibly cause the liquid core to oscillate within the subchannel. This rapid increase could be due to phenomena such as that observed in the microbreaking wave regime described by Banerjee & MacIntyre [19] for mass transfer at the ocean surface. As there is no experimental information on the vapor velocity for this region, it would be difficult to develop a model based on data. However, as the subcooling is low, the interfacial heat transfer rate is also low and so an approximate model would suffice.

The effect of the pressure on the asymptotic value of the liquid-side Nusselt number was addressed above for the RBHT reflood data. Using the minimum film boiling point data analysis procedure, estimates of $Nu_{li}$ were obtained for pressures up to 9 MPa. Both measured values and these estimated values are plotted as a function of the liquid Prandtl number in Figure 10 below. Although some of the high-pressure estimated values are low, most of the points are reasonably well fit by

$$Nu_{li} = 130\cdot Pr_l^{1/2} \quad (10)$$

and so equation (10) is proposed for the thermally controlled region.

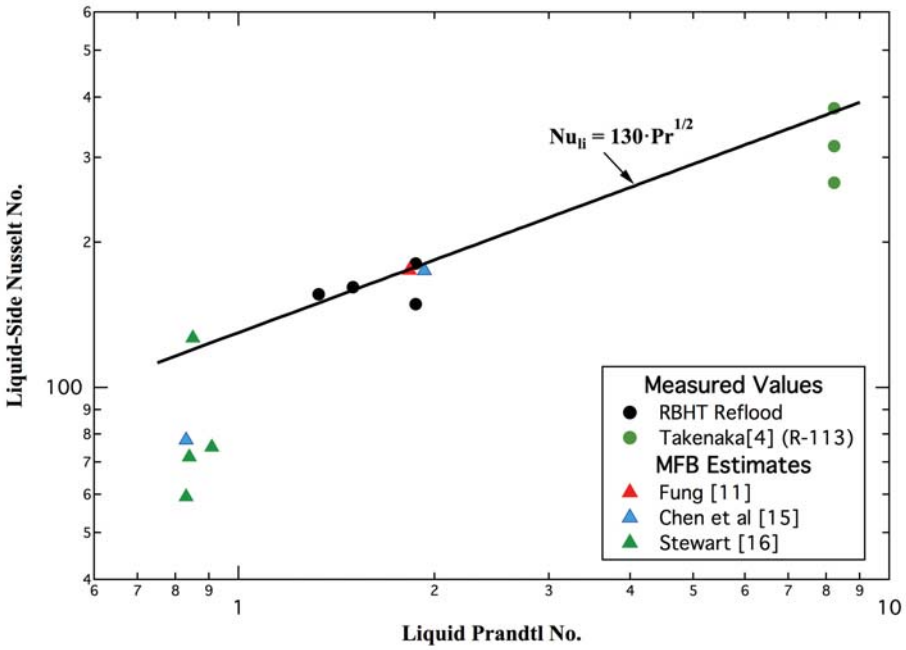


**Figure 10. Behavior of the asymptotic value of the liquid-side Nusselt number with Prandtl number.**

For direct contact condensation on the surface of coherent liquid jets, the interfacial heat transfer is a strong function of the turbulence level in the jet and hence of the liquid Reynolds number upstream of the jet discharge. As the flow topology of the inverted annular liquid core resembles that of a liquid jet, albeit with a discharge directed vertically upwards, a strong mass flux effect would be expected for the liquid-side Nusselt number as well.

To investigate this effect, estimates obtained from the supplemental data analysis procedures described in the previous section were used to extend the mass flux range as shown in Figure 11. For all of the data sets where the mass flux was less than about 1000 (kg/m$^2$s), corresponding to a liquid Reynolds number of up to 9x10$^4$, there was no evidence of any dependence upon the mass flux. Indeed, only the minimum film boiling data of Stewart [16] at 9 MPa showed any effect. For this data set, the inferred value of $Nu_{li}$ increased by a factor of 3 as the mass flux increased from 930 to 2750 (kg/m$^2$s) and had a value of the Nusselt number close to that expected for turbulent convection. This suggests that, once some threshold has been reached, the turbulence level in the liquid core generated by wall shear upstream of the quench front may govern the liquid-side interfacial heat transfer in the IAFB regime. However, this one data point is not sufficient to reach such a conclusion. Points in Figure 11 for which the estimated value of the Nusselt number is below that for turbulent convection could be due to either the magnitude of the experimental error or to damping of the turbulence within the liquid core by the free surface.

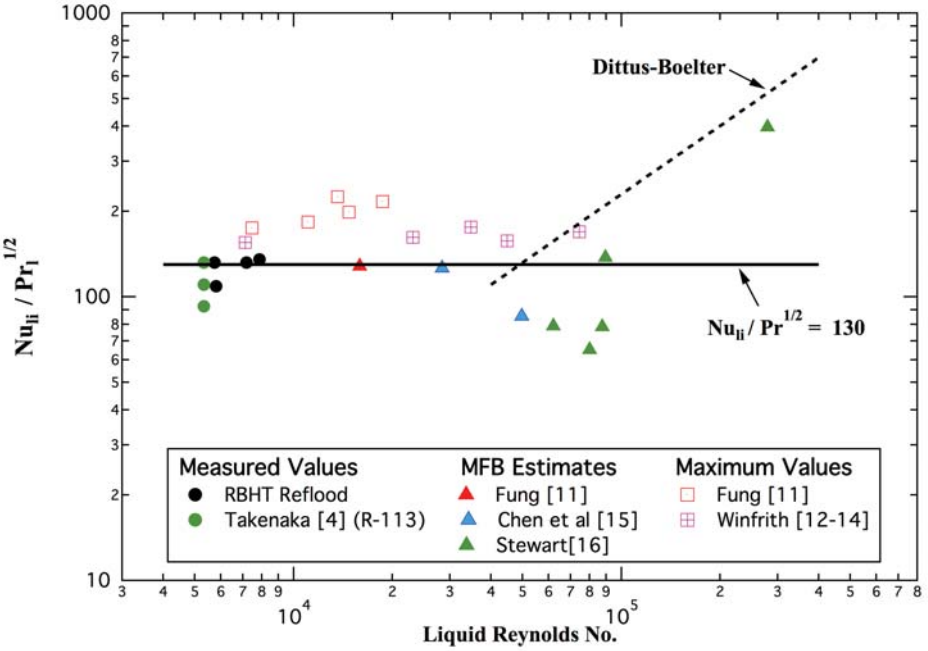


**Figure 11. Behavior of the liquid-side Nusselt number vs. the liquid Reynolds number.**

## 6. SUMMARY

An analysis procedure was developed to deduce values for the liquid-side Nusselt number in the IAFB regime from the fluid thermocouple measurements during transient reflood tests conducted in the RBHT facility. A Lagrangian frame of reference moving with the quench front was used to translate the measured temperature histories into axial profiles of the liquid subcooling for the inverted annular column. From a heat balance on the liquid core, the interfacial heat transfer rate and corresponding Nusselt number were determined.

In contrast to typical models used in two-fluid analysis codes, no entrance length effect was observed for the liquid-side Nusselt number. Rather, $Nu_{li}$ was at its minimum value for the highly subcooled region just downstream of the quench front. Further downstream, as the liquid subcooling was reduced and the vapor flow rate increased, the Nusselt number increased dramatically as the waviness of the interface increased. Part of this enhancement was explained by the augmentation of the turbulence level within the liquid column due to interfacial shear. A slight decrease in the Nusselt number was observed as the pressure increased but the effect was of the same order as the uncertainty in the measurements.

Two supplementary data analysis procedures were developed to infer estimates for the value of the liquid-side Nusselt number from film boiling experiments where the interfacial heat transfer was not measured. This allowed the database to be extended to both high-pressure and high mass flux conditions. The decrease in $Nu_{li}$ with pressure seen in the RBHT experiments was confirmed and tentatively correlated with the liquid Prandtl number. No effect of the mass flux was observed for values below 1000 ($kg/m^2s$). Only one set of data, at a mass flux of 2750 ($kg/m^2s$), showed the dependence of the Nusselt number upon liquid Reynolds number expected for turbulent convection. To clarify these parametric effects and reduce the uncertainty in the interfacial heat transfer model in the USNRC's TRACE thermal-hydraulic analysis code, a small-scale experimental program is being planned.

## NOMENCLATURE

| | | | |
|---|---|---|---|
| A | : flow area | $U_i$ | : interfacial friction velocity $(\tau_i/\rho_l)^{1/2}$ |
| $A_i$ | : interfacial area | V | : velocity |
| $C_P$ | : specific heat | Z | : axial distance |
| $D_c$ | : diameter of subcooled liquid core | $\alpha$ | : void fraction |
| $D_h$ | : hydraulic diameter | $\rho$ | : density |
| G | : mass flux | | |
| h | : heat transfer coefficient | *Subscripts* | |
| k | : thermal conductivity | *l, liq* | : liquid phase |
| K | : mass transfer coefficient | *li* | : liquid-interface |
| Nu | : Nusselt number | *min* | : minimum film boiling point |
| Pr | : Prandtl number | *QF* | : quench front |
| q" | : heat flux | *sat* | : saturation |
| Q | : heat flow rate | *sub* | : subcooling |
| Re | : Reynolds number | *v* | : vapor |
| Sc | : Schmidt number | *vi* | : vapor-interface |
| t | : time | *w* | : wall |
| T | : temperature | *wv* | : wall-vapor |

## REFERENCES


1. R. Vijaykumar and V.K. Dhir, "An Experimental Study of Subcooled Film Boiling on a Vertical Surface – Hydrodynamic Aspects," *J. of Heat Transfer*, **114**, pp. 161-168 (1992).
2. R. Vijaykumar and V.K. Dhir, "An Experimental Study of Subcooled Film Boiling on a Vertical Surface – Thermal Aspects," *J. of Heat Transfer*, **114**, pp. 169-178 (1992).
3. N. Takenaka, T. Fujii, K. Akagawa and K. Nishida, "Flow Pattern Transition and Heat Transfer of Inverted Annular Flow," *Int. J. Multiphase Flow*, **15**, pp. 767-785 (1989).
4. N. Takenaka, K. Akagawa, T. Fujii and K. Nishida, "Experimental Study of Flow Pattern and Heat Transfer of Inverted Annular Flow," *Nuclear Engineering and Design*, **120**, pp. 293-300 (1990).
5. M. Aritomi, A. Inoue, S. Aoki and K. Hanawa, "Thermo-Hydraulic Behavior of Inverted Annular Flow," *Nuclear Engineering and Design*, **120**, pp. 281-291 (1990).
6. P.K. Meduri, "Wall Heat Flux Partitioning During Subcooled Flow Film Boiling of Water on a Vertical Surface," *Ph.D. thesis*, Dept. of Mechanical Engineering, University of California, Los Angeles, CA (2007).
7. E.R. Rosal et al., "Rod Bundle Heat Transfer Test Facility Description," NUREG/CR-6976, (2008).
8. L.E. Hochreiter et al., "RBHT Reflood Heat Transfer Experiments Data and Analysis," NUREG/CR-6980, (2012).
9. G. Costigan and C.D. Wade, "Visualization of the Reflooding of a Vertical Tube by Dynamic Neutron Radiography," *International Workshop on Post-Dryout Heat Transfer*, Salt Lake City, UT, NUREG/CP-0060, (1984).
10. US Nuclear Regulatory Commission, "*TRACE V5.0 Theory Manual: Field equations, Solution methods, and Physical models*", ADAMS accession no. ML120060218 (2007).
11. K.K. Fung, "Subcooled and Low Quality Film Boiling of Water in Vertical Flow at Atmospheric Pressure," *Ph. D. Thesis*, University of Ottawa, Canada (1981).
12. D. Swinnerton, M.L. Hood and K.G. Pearson, "Steady State Post-Dryout Experiments at Low Quality and Medium Pressure," UKAEA Report, AEEW-R-2267 (1988).
13. R.A Savage, D. Archer and D. Swinnerton, "Heat Transfer and Voidage Measurements in Steady State Post-Dryout at Low Quality and High Pressure," *IChemE 3rd UK National Heat Transfer Conference*, Birmingham, UK, Vol. 1, pp. 607-615 (1992).
14. R.A Savage, D. Archer and D. Swinnerton, "Flow Visualization, Heat Transfer, and Voidage Measurements in Steady State Post-Dryout at High Pressure," *Proceedings of NURETH-6*, Grenoble, France, Vol. 2, pp. 1311-1318 (1993).
15. Y. Chen et al., "Experimental Measurement of the Minimum Film Boiling Temperature for Flowing Water," *Multiphase Flow and Heat Transfer; 2nd International Symposium*, Vol. 1, pp. 393-400 (1989).
16. J.C. Stewart, "Low Quality Film Boiling at Intermediate and Elevated Pressures," *M.S. Thesis*, University of Ottawa, Canada (1981).
17. P. Saha and N. Zuber, "Point of Net Vapor Generation and Vapor Void Fraction in Subcooled Boiling," *Proceedings of 5th International Heat Transfer Conference*, Tokyo, Japan, Vol. IV, pp. 175-179 (1974).
18. V. DeAngelis et al., "Microphysics of Scalar Transfer at Air-Water Interfaces," in *Proceedings of Wind-Over-Wave Couplings: Perspectives and Prospects*, Oxford University Press, Oxford (1997).
19. S. Banerjee and S. MacIntyre, "The Air-Water Interface: Turbulence and Scalar Exchange," in *Advances in Coastal and Ocean Engineering*, World Scientific, Hackensack, N.J., USA, Vol. 9, pp. 181-237 (2004).
20. M. Takahashi et al., "Experimental Study on Condensation Heat Transfer on Surface of Liquid Jet," J. Nuclear Science and Technology, 29, pp. 721-734, 1992.